

REFLECTIVE HYPERBOLIC 2-ELEMENTARY LATTICES, K3 SURFACES AND HYPERKAHLER MANIFOLDS

VALERY ALEXEEV

ABSTRACT. We compute Coxeter diagrams of several “large” reflective 2-elementary even hyperbolic lattices and their maximal parabolic subdiagrams, and give some applications of these results to the theory of K3 surfaces and hyperkahler manifolds.

CONTENTS

1. Introduction	2
2. Definitions and notations	4
3. Coxeter diagrams and maximal parabolic subdiagrams	6
(11, 11, 1)	7
(12, 10, 1)	8
(13, 9, 1)	8
(14, 8, 0)	8
(14, 8, 1)	8
(15, 7, 1)	8
(16, 6, 1)	9
(18, 4, 0)	11
(20, 2, 1)	12
(13, 11, 1)	12
(14, 10, 1)	12
(15, 9, 1)	12
(18, 6, 0)	13
(22, 2, 0)	13
(14, 12, 1)	13
(15, 11, 1)	13
(15, 13, 1)	14
(16, 12, 1)	14
(16, 14, 1)	14
Other coeven lattices	14
4. Applications to infinite automorphism groups of K3 surfaces	14
References	16

Date: June 10, 2023.

2010 *Mathematics Subject Classification.* 14J28, 20F55.

1. INTRODUCTION

Even hyperbolic lattices L appear in the theory of K3 surfaces and hyperkahler manifolds in several ways:

(1) As the Picard lattice S_X of a K3 surface X together with the intersection form, resp. as the Picard lattice $S_X \subset H^2(X, \mathbb{Z})$ of a hyperkahler manifold X , with the Beauville-Bogomolov-Fujiki form. In this interpretation, the primitive isotropic vectors $v \in S_X$, $v^2 = 0$, correspond to elliptic, resp. Lagrangian fibrations.

(2) As the hyperbolic lattice δ^\perp/δ attached to a 0-cusp of the moduli space of lattice polarized K3 surfaces, resp. hyperkahler manifolds. In this interpretation, the isotropic vectors correspond to 1-cusps of the moduli space and to Type II degenerations. (Here, δ is an isotropic vector in some lattice H of signature $(2, n)$ for some n , defining a 0-cusp; then δ^\perp/δ has signature $(1, n - 1)$.)

Let L be such a lattice. Since we are mostly concerned with application to algebraic geometry, “hyperbolic” for us means signature $(1, r - 1)$. The isometry group $O(L)$ contains two important normal subgroups $W_2(L)$ and $W_r(L)$ generated by reflections in the (-2) -vectors, resp. in all reflective vectors $r \in L$ with $r^2 < 0$. They are described by the Coxeter diagrams Γ_2 , resp. Γ_r . The lattice is called 2-reflective, resp. reflective if $W_2(L)$, resp. $W_r(L)$ has finite index in $O(L)$.

By the Torelli theorem, the automorphism group $\text{Aut}(X)$ of a K3 surface is commensurable to $O(S_X)/W_2(S_X)$, in particular $\text{Aut}(X)$ is finite iff S_X is 2-reflective. In some cases when S_X is not 2-reflective but is reflective, the Coxeter diagram Γ_r provides a nice description of the infinite group $\text{Aut}(X)$, see Vinberg [Vin83] for a classical example. In the case of hyperkahler manifolds, similar results hold for the group $\text{Bir}(X)$ of birational automorphisms. In the second interpretation above, reflective lattices provide toroidal compactifications of the moduli spaces.

A simple but very powerful way to compute the Coxeter diagrams Γ_2 and Γ_r is Vinberg’s algorithm [Vin72, Vin75]. When the lattice is 2-reflective, resp. reflective, the algorithm completes in finitely many steps. Then the $O(L)$ -orbits of primitive isotropic vectors correspond to the maximal parabolic subdiagrams.

In this paper we treat the case of 2-elementary lattices, i.e. the lattices with $L^*/L \simeq \mathbb{Z}_2^a$. By Nikulin [Nik79] an indefinite even 2-elementary lattice is uniquely determined by its signature and a triple of integers (r, a, δ) , where r is its rank, $a \equiv r \pmod{2}$ is the \mathbb{Z}_2 -rank, and $\delta \in \{0, 1\}$ is a certain invariant which we call coparity. In the case of K3 surfaces, these are the generic Picard lattices of K3 surfaces with a nonsymplectic involution.

In some sense 2-elementary lattices are one step up from unimodular lattices. For such lattices Γ_2 is easily derived from Γ_r , even if one or both of these diagrams are infinite, cf. [Vin83, Prop. on p.2] or [AN06, Prop. 2.4]. In any case, Γ_r is usually dramatically smaller than Γ_2 , so it is a good strategy to compute Γ_r .

To begin with, there are only finitely many reflective 2-elementary lattices. Indeed, $a \leq r$, and by Esselmann [Ess96] a reflective lattice satisfies $r \leq 20$ or $r = 22$. For lattices with $r + a \leq 18$ the Coxeter diagrams Γ_r were computed by Nikulin in [AN06, Table 1]. For $r + a = 20$ we computed them in [AE22]. The latter paper also contains a description of the isotropic vectors for $r + a \leq 20$.

For K3 surfaces over \mathbb{C} the Picard lattice satisfies $r + a \leq 22$. The initial motivation for this paper was to classify the reflective diagrams Γ_r with $r + a = 22$ and to compute the maximal parabolic subdiagrams in them.

The diagrams for $(11, 11, 1)$, $(12, 10, 1)$, $(13, 9, 1)$, $(14, 8, 0)$ and $(14, 8, 1)$ are relatively small and we give them in Figure 3. The others are too large to draw directly. However, it turns out that they are remarkably symmetric and can be described in a way similar to the papers [VK78, Vin83] of Vinberg and Kaplinskaja.

Theorem 1.1. *The 2-elementary lattices $(17, 5, 1)$, $(18, 4, 1)$ and $(19, 3, 1)$ are not reflective. The other even 2-elementary lattices on the line $r + a = 22$ are reflective.*

Definition 1.2. Let G be a graph and $n \geq 2$ be an integer. Define the edge n -fold graph $G^{(n)}$ by subdividing each edge of G into n edges and inserting $n - 1$ intermediate vertices. Thus, $G^{(n)}$ has $n|E_G|$ edges and $|V_G| + (n - 1)|E_G|$ vertices.

We note that the vertices of $G^{(2)}$ are in a natural bijection with the set of vertices and edges of G .

Definition 1.3. We say that a diagram Γ is built on top of a simple graph H if it contains a subdiagram of the *main roots* isomorphic to H , and the *additional roots* are defined in terms of the main roots by some specified rules. For the 2-elementary lattices of this paper the main roots are the (-2) -roots α in L of divisibility 1, i.e. satisfying $\alpha \cdot L = \mathbb{Z}$. For the lattices in Theorem 1.4 the following is also true: if a main root α and an additional root β are connected then $\alpha \cdot \beta = 2$.

Theorem 1.4. *For $n = 3, 4, 5, 6$ the Coxeter diagram Γ_r of the even 2-elementary lattice $(10 + n, 12 - n, 1)$ is built on top of $G^{(2)}$, where $G = K_n$ is the complete graph on n vertices. The diagram Γ_r for $(18, 4, 0)$ is built on top of $G^{(2)}$, where $G = K_{4,4}$ is the complete bipartite graph on 8 vertices, and that of $(14, 8, 0)$ on top of $G^{(2)}$ for $G = D_4$. In all cases one has $\text{Aut } \Gamma_r = \text{Aut } G$ and $O^+(S) = \text{Aut } G \ltimes W_r$.*

In some cases, e.g. $(11, 11, 1)$, $(18, 4, 0)$, $(20, 2, 1)$, the diagrams were previously known. We add the computations of the maximal parabolic diagrams, which are not easy to extract from the literature.

We also investigated the remaining finitely many possibly reflective 2-elementary lattices. Some of these lattices appear as the Picard lattices of hyperkahler manifolds of $K3^{[2]}$ -type. Indeed if X is a K3 surface then $S(\text{Hilb}^n X) = \langle 2 - 2n \rangle \oplus S_X$. In particular, if S_X is 2-elementary then $S(\text{Hilb}^2 X) = \langle -2 \rangle \oplus S_X$ is also 2-elementary. The lattice $(15, 9, 1) = \langle -2 \rangle \oplus (14, 8, 1)$ below provides such an example with a very interesting automorphism group, possibly related to the Klein quartic.

There are similar identities for the hyperkahler manifolds of Kummer and OG6 types, but those lattices are quite small. (In the OG10 type the Picard lattices are of the form $A_2 \oplus S_X$ and so are not 2-elementary since $A_2^*/A_2 = \mathbb{Z}_3$.)

And some of the bigger lattices appear on K3 surfaces and hyperkahler manifolds in positive characteristic, for example the lattice $(22, 2, 0)$ investigated by Dolgachev and Kondō [DK03].

We prove the following (for the converse, see Remark 3.1):

Theorem 1.5. *The even hyperbolic 2-elementary lattices of Fig. 1 are reflective.*

It is interesting to compare the diagrams on the $r + a = 22$ line with those on the $r + a = 20$ line, computed in [AE22, Sec. 3]. The latter are smaller but less symmetric: they have the dihedral symmetry of n -gons. Most diagrams for $r + a \leq 18$ do not have any symmetries at all.

The diagrams on the line $r + a = 20$ turn out to be key to understanding degenerations of K3 surfaces with a nonsymplectic involution via a mirror symmetry

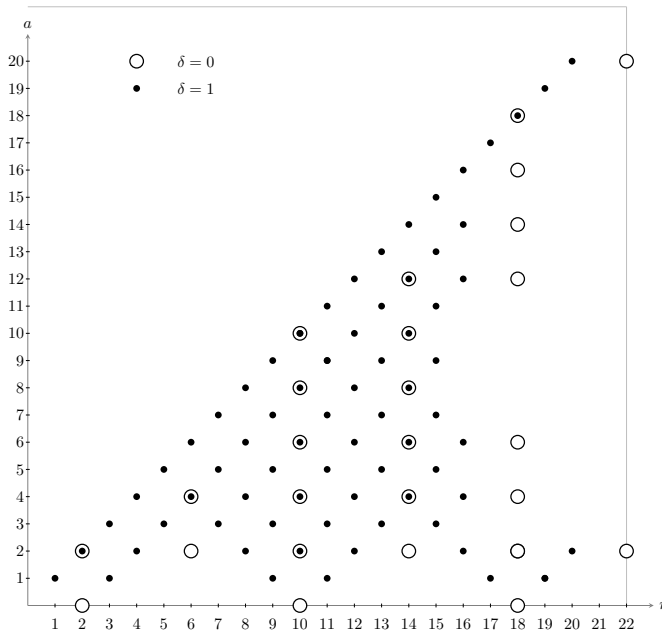


FIGURE 1. Reflective even hyperbolic 2-elementary lattices

construction. The lattices with $r + a \geq 22$ do not appear as targets of the mirror symmetry correspondence of the ordinary K3 surfaces. But they may appear on the mirrors of higher-dimensional hyperkahler manifolds. What do the symmetries of the Coxeter diagrams imply about their degenerations?

The organization of the paper is as follows. In Section 2 we recall some standard definitions and fix the notations. In Section 3 we prove the above theorems and give detailed descriptions of the Coxeter diagrams and their maximal parabolic subdiagrams. In Section 4 we give some applications to the infinite automorphism groups of K3 surfaces.

Acknowledgements. I am grateful to Boris Alexeev for help at critical points in my computations. I thank Professors Kondō and Mukai for useful discussions. I was partially supported by the NSF grant DMS-2201222.

2. DEFINITIONS AND NOTATIONS

A lattice is a group $S \simeq \mathbb{Z}^r$ together with a nondegenerate \mathbb{Z} -valued symmetric bilinear form. It is even if x^2 is even for all $x \in S$. It is 2-elementary if $A_S := S^*/S \simeq \mathbb{Z}_2^a$ for some $a \geq 0$, where $S^* \subset S \otimes \mathbb{Q}$ is the dual group. Because we are coming from the algebraic geometry direction, for us a hyperbolic lattice of rank r has signature $(1, r - 1)$. A reflection in a vector $\alpha \in S$ is the linear transformation

$$w_\alpha(v) = v \rightarrow v - 2 \frac{v \cdot \alpha}{\alpha^2} \alpha.$$

A root is a vector $\alpha \in S$ such that $\alpha^2 < 0$ and $w_\alpha(S) = S$. In an even 2-elementary lattice the roots are the (-2) vectors and the (-4) -vectors of divisibility 2. The divisibility $\text{div}(\alpha)$ is defined by $\alpha \cdot S = \text{div}(\alpha)\mathbb{Z}$.

The reflections in the (-2) -vectors generate the group $W_2(S)$, and the reflections in all roots, in our case the (-2) - and (-4) -roots, generate a bigger group $W_r(S)$. Both are normal subgroups of the isometry group $O(S)$, and also of its index-2 subgroup $O^+(S)$ preserving the light cone. The lattice is called 2-reflective, resp. reflective if these subgroups have finite index.

A_n, D_n, E_n denote the standard root lattices generated by (-2) -roots, and they are *negative definite*. $U = \begin{pmatrix} 0 & 1 \\ 1 & 0 \end{pmatrix}$ denotes the hyperbolic plane. For any lattice H , $H(n)$ denotes the same group with the product $x \cdot y$ in $H(n)$ equal to $nx \cdot y$ in H . For the 2-elementary lattices with short (-2) and long (-4) -roots additionally there are root lattices $B_n(2)$, C_n and F_4 . Considered as the (-2) -root lattices, they are A_1^n , D_n , and D_4 respectively.

By [Nik79] an indefinite even 2-elementary lattice is uniquely determined by its signature and a triple of integers (r, a, δ) , where r is its rank, a is the \mathbb{Z}_2 -rank, and $\delta \in \{0, 1\}$ is an invariant which we call coparity, see [AE22, Def. 2.4, Lem. 2.5]. A 2-elementary lattice S is coeven ($\delta = 0$) if the doubled dual $S^\dagger := S^*(2)$ is even, and it is coodd ($\delta = 1$) if S^\dagger is odd. A direct sum of 2-elementary lattices is coeven iff so is every summand.

Any even hyperbolic 2-elementary lattice is a direct sum of one of the elementary hyperbolic summands $\langle 2 \rangle$, U , $U(2)$ with $(r, a, \delta) = (1, 1, 1)$, $(2, 0, 0)$, $(2, 2, 0)$ respectively, and a direct sum of the following elliptic root lattices for the full reflection group, which we list with their (r, a, δ) . $B_n(2) : (n, n, 1)$, $C_{4n} : (4n, 2, 0)$ for $4n \geq 8$, $C_{4n+2} : (4n+2, 2, 1)$ for $4n+2 \geq 6$, $F_4 : (4, 2, 0)$, $E_7 : (7, 1, 1)$, $E_8 : (8, 0, 0)$, and $E_8(2) : (8, 8, 0)$.

We refer to [Vin72] for Vinberg's theory. We use the notations of that paper for elliptic and parabolic Coxeter diagrams. The vertices of Γ_r denote the roots α_i orthogonal to the facets of the fundamental polyhedron P_r . The types of edges specify the angle θ between α_i, α_j . A single line means $\theta = \pi/3$, double line $\theta = \pi/4$, no line $\theta = \pi/2$, a bold line means that the hyperplanes defining the two facets meet at an infinite point of the hyperbolic space \mathcal{H} , and a broken line means that they are skew.

For a 2-elementary lattice, we denote the short, (-2) -roots by white vertices and the long, (-4) -roots by black vertices. Then the types of edges correspond to the following intersection numbers $\alpha_i \cdot \alpha_j$ between the roots:

α_i^2	α_j^2	simple	double	bold	broken
-2	-2	1		2	> 2
-4	-4	2		4	> 4
-2	-4		2		> 2

The parabolic $\tilde{A}_n, \tilde{D}_n, \tilde{E}_n$ diagrams could consist either of all short, or of all long roots. In the latter case we denote them $\tilde{A}_n(2), \tilde{D}_n(2), \tilde{E}_n(2)$. If this parabolic subdiagram $\Gamma \subset \Gamma_r$ corresponds to a vector $v \in S$ with $v^2 = 0$ then its image in v^\perp/v spans an elliptic root system. For all white vertices it is A_n, D_n, E_n , and for all black vertices it is $A_n(2), D_n(2), E_n(2)$.

Similarly, for \tilde{B}_n, \tilde{C}_n and \tilde{F}_4 there are two versions, *short* and *long*, which are dominated by the short, resp. long roots. We list them in Figure 2, together with the elliptic root lattices v^\perp/v . Here, “dominated” means that they form the majority

of roots “for large n ”. For example for \tilde{C}_n the short roots start to dominate only for $n \geq 4$. One should keep in mind that $D_2 = A_1^2$ and $D_3 = A_3$.

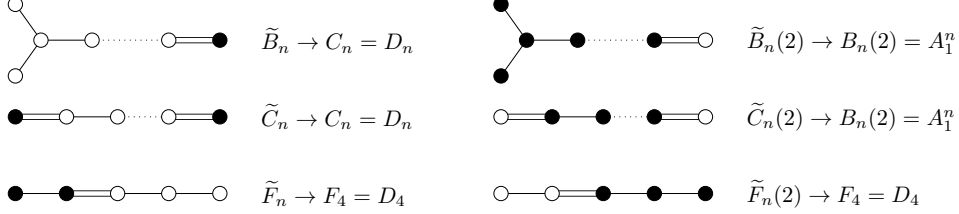


FIGURE 2. Extended Dynkin diagrams dominated by short or long vectors

By [AE22, Prop. 5.5] the primitive isotropic vectors $v \in S$, $v^2 = 0$ are of three types. Denoting $\bar{S} = v^\perp/v$ and with v a vector in the first summand, the types are:

- (1) (odd) $S = U \oplus \bar{S}$, $a_{\bar{S}} = a_S$, $\delta_{\bar{S}} = \delta_S$.
- (2) (even ordinary) $S = U(2) \oplus \bar{S}$, $a_{\bar{S}} = a_S - 2$, $\delta_{\bar{S}} = \delta_S$.
- (3) (even characteristic) $S = I_{1,1}(2) \oplus \bar{S}$, $a_{\bar{S}} = a_S - 2$, $\delta_S = 1$ and $\delta_{\bar{S}} = 0$.

Thus, classifying isotropic vectors in an even hyperbolic 2-elementary lattice with the invariants (r, a, δ) is equivalent to classifying the even negative definite lattices \bar{S} with the invariants $(r - 2, a, \delta)$, $(r - 2, a - 2, \delta)$ and $(r - 2, a - 2, 0)$.

3. COXETER DIAGRAMS AND MAXIMAL PARABOLIC SUBDIAGRAMS

Proof of Thm. 1.5. For some of these lattices the Coxeter diagrams are well known: for those on the $a = 0$ line (they are unimodular) and for those on the $r = a$ line (they are twice the unimodular). The two hardest cases were done by Vinberg and Kaplinskaja [VK78].

For others we performed the computation following Vinberg’s algorithm. Each of these lattices can be written as $U \oplus \Lambda$ or $U(2) \oplus \Lambda$ for some root lattice Λ , where U is the hyperbolic plane. We chose the control vector to be a vector v_0 in the first summand, with $v_0^2 = 2$ for U , resp. $v_0^2 = 4$ for $U(2)$, and ran the algorithm using a custom Sage [Sag22] script written for this purpose.

We checked the completeness of the diagrams directly, by confirming that the cones in the Minkowski spaces $\mathbb{R}^{1, r-1}$ defined by the roots of Γ_r lie entirely in \bar{C} .

For the diagrams without broken edges the easy sufficient condition of [Vin75] also works to verify the completeness by hands: the diagrams do not contain Lannér subgraphs, and every connected parabolic subdiagram is contained in a maximal parabolic subdiagram of maximal rank. For the diagrams with broken edges, the criterion of [Vin72, Prop. 2] works. \square

Proof of Thm. 1.4. This follows by observation, analyzing the Coxeter diagrams produced by the above method. \square

Proof of Thm. 1.1. For the nonreflective lattices the proof is as follows. One has

$$(19, 3, 1) = \langle -2 \rangle \oplus (18, 2, 1) \text{ and } (18, 4, 1) = \langle -2 \rangle \oplus (17, 3, 1).$$

The fundamental polyhedron $P_r(18, 2, 1)$ is a face of $P_r(19, 3, 1)$ and $\Gamma_r(18, 2, 1)$ is smaller than $\Gamma_r(19, 3, 1)$, see [AE22, Lem. 4.14]. Similarly for $(18, 4, 1)$. The

diagrams $\Gamma_r(18, 2, 1)$, $\Gamma_r(17, 3, 1)$ are infinite by [AE22, Thm. 3.6], and so are $\Gamma_r(19, 3, 1)$ and $\Gamma_r(18, 4, 1)$.

Finally, one has $(17, 5, 1) \simeq U(2) \oplus \Lambda$ for any even 2-elementary negative definite lattice Λ with $(r, a, \delta) = (15, 3, 1)$, where U is a hyperbolic plane. If the lattice $(17, 5, 1)$ were reflective then Λ would correspond to a maximal parabolic subdiagram of Γ_r and the root sublattice $R(\Lambda)$ would have rank equal to $r(\Lambda) = 15$. But by [AE22, Table 2] there exists Λ with $R(\Lambda) = A_{13}A_1(2)$ of rank 14. \square

Remark 3.1. From the experimental data, it appears that the list of reflective 2-elementary lattices given in Fig. 1 may be complete. For many, but not all of the missing nodes the non-reflectivity can be checked by using the duality $L \rightarrow L^\dagger$ and the arguments as in the proof of Theorem 1.1.

Next, we list the Coxeter diagrams of Fig. 1 with $r + a \geq 22$ and the maximal parabolic diagrams in them. The diagrams for the lattices $(11, 11, 1)$, $(12, 10, 1)$, $(13, 9, 1)$, $(14, 8, 0)$ and $(14, 8, 1)$ are shown in Figure 3.

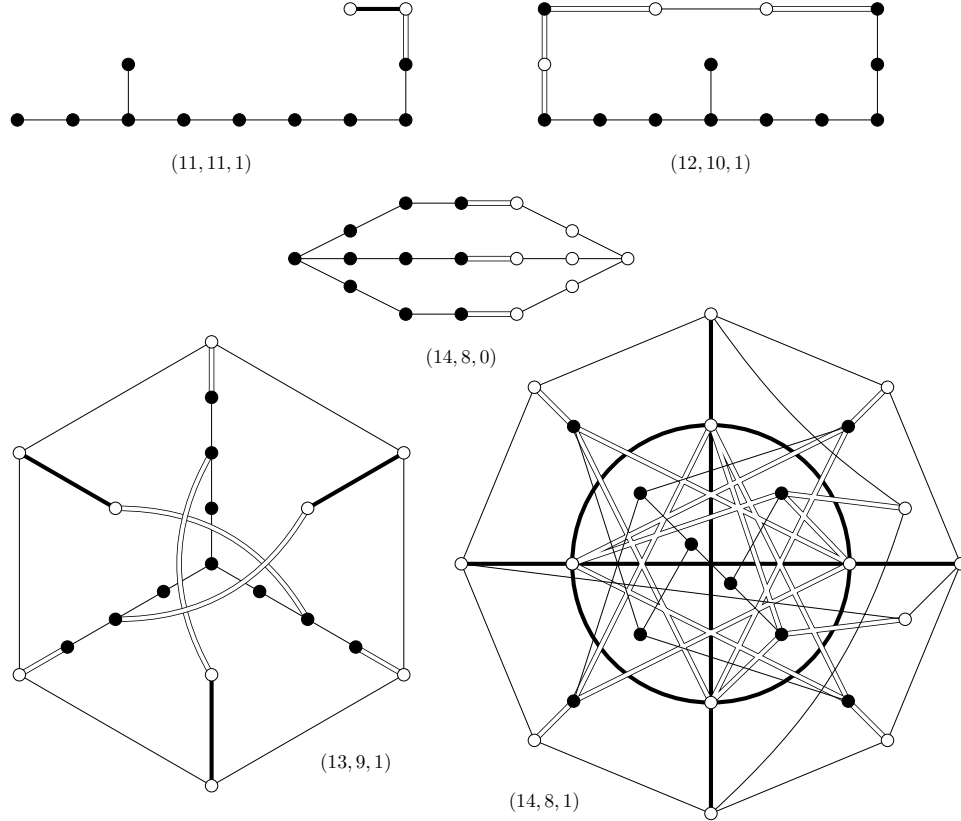


FIGURE 3. Coxeter diagrams Γ_r for ranks $r \leq 14$

(11, 11, 1). Γ_r has 12 roots. There are two isotropic vectors v modulo $O^+(S)$. They correspond to the following subdiagrams of the Coxeter diagram, both even ordinary: $\tilde{E}_8(2)\tilde{A}_1$ and $\tilde{B}_9(2)$. The automorphism group of Γ_r is trivial.

(12, 10, 1). Γ_r has 14 roots. Note that for the parabolic subdiagram \tilde{C}_3 the corresponding root lattice v^\perp/v is $C_3 = D_3 = A_3$. There are 5 maximal parabolic subdiagrams listed below. The automorphism group of Γ_r is trivial.

- (1) odd: $\tilde{E}_8(2)\tilde{C}_2(2), \tilde{C}_{10}(2)$.
- (2) even ordinary: $\tilde{E}_7(2)\tilde{C}_3, \tilde{B}_6(2)\tilde{F}_4(2), \tilde{B}_8(2)\tilde{C}_2$.

(13, 9, 1). Γ_r has 19 roots. There are 22 maximal parabolic subdiagrams, and 7 modulo $\text{Aut } \Gamma_r = S_3$:

- (1) odd: $\tilde{C}_8(2)\tilde{C}_3(2), \tilde{E}_7(2)\tilde{B}_3\tilde{A}_1, \tilde{C}_7(2)\tilde{F}_4$.
- (2) even ordinary: $\tilde{F}_4^2(2)\tilde{B}_3(2), \tilde{C}_6\tilde{B}_5(2), \tilde{B}_6(2)\tilde{C}_4\tilde{A}_1, \tilde{E}_6(2)\tilde{A}_5$.

It is clear that this diagram is built on top of the graph $K_3^{(2)}$. The main roots are the 6 roots on the outside hexagon, and the additional roots come in four layers culminating with the central vertex. The roots generate the lattice, so the S_3 -action on Γ_r extends to the action on the lattice H itself.

(14, 8, 0). Γ_r has 17 roots. There are 11 maximal parabolic subdiagrams, and 5 modulo $\text{Aut } \Gamma_r = S_3$:

- (1) odd: $\tilde{E}_7(2)\tilde{B}_5, \tilde{C}_8(2)\tilde{F}_4$.
- (2) even ordinary: $\tilde{F}_4^3(2), \tilde{C}_6\tilde{B}_6(2), \tilde{E}_6\tilde{E}_6(2)$.

It is clear that this diagram is built on top of the graph $D_4^{(2)}$, where D_4 is a tree with four vertices, the central vertex of degree 3 and three ends.

(14, 8, 1). Γ_r has 24 roots. There are 127 maximal parabolic subdiagrams, and 15 modulo $\text{Aut } \Gamma_r = S_4$:

- (1) odd: $\tilde{F}_4^2\tilde{C}_4(2), \tilde{B}_6\tilde{C}_6(2), \tilde{C}_6(2)\tilde{B}_4\tilde{C}_2(2), \tilde{E}_6(2)\tilde{A}_5\tilde{A}_1, \tilde{D}_6(2)\tilde{B}_3^2, \tilde{C}_4^3(2)$.
- (2) even ord: $\tilde{C}_6\tilde{F}_4(2)\tilde{C}_2, \tilde{C}_4^2\tilde{B}_4(2), \tilde{D}_6\tilde{B}_5(2)\tilde{A}_1, \tilde{E}_7\tilde{B}_5(2), \tilde{C}_8\tilde{B}_4(2), \tilde{A}_7\tilde{D}_5(2)$.
- (3) even char: $\tilde{F}_4^3(2), \tilde{C}_6\tilde{B}_6(2), \tilde{E}_6\tilde{E}_6(2)$.

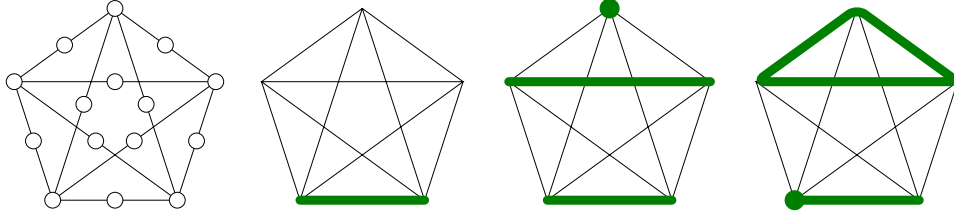
It is clear that this diagram is built on top of the graph $K_4^{(2)}$. Denote the main roots α_i^m with $i = 1, 2, 3, 4$ for the 4 vertices and α_{ij}^m with $1 \leq i < j \leq 4$ for the 6 edges of K_4 . For each edge there is an additional (-2) -root α_{ij} attached to it, and a (-4) -root α_{ij}^+ attached to α_{ij} . One has $\alpha_{ij}^m \cdot \alpha_{ij} = \alpha_{ij} \cdot \alpha_{ij}^+ = 2, \alpha_{ij}^m \cdot \alpha_{ij}^+ = 0$. Let $\bar{\alpha}_{ij} = \alpha_{ij} + \alpha_{ij}^+$.

Then the 12 roots $\alpha_{ij}, \bar{\alpha}_{ij}$ are mutually orthogonal, and are also orthogonal to the central (-4) -root α_{cen} . The orthogonal complement of these 13 vectors in H is $\mathbb{Z}h$ with $h = \frac{1}{2}(\sum \alpha_i^m + \sum \alpha_{ij} + \sum \bar{\alpha}_{ij})$. One has $h^2 = 4$. Set $e = \frac{1}{2}(h + \alpha_{cen})$ and $f = \frac{1}{2}(h - \alpha_{cen})$. Then the 14 vectors $\alpha_{ij}, \bar{\alpha}_{ij}, e, f$ form the standard basis of a sublattice of H isomorphic to $(I_{0,12} \oplus U)(2)$. Thus, H can be identified with an S_4 -invariant lattice lying between it and its dual $(I_{0,12} \oplus U)(\frac{1}{2})$.

Picking $v_0 = h$ to be the control vector, Vinberg's algorithm ends in two steps.

(15, 7, 1). Γ_r contains 60 roots. As in Definition 1.3, it is built on top of the graph $K_5^{(2)}$. The subdiagram of the main roots is $K_5^{(2)}$, as shown on the left in Fig. 4. The 15 main roots form a basis of the lattice.

Recall Definition 1.2 of the graph $G^{(2)}$. The vertices of $G^{(2)}$ are naturally in a bijection with the set of vertices + edges of G . Using this bijection, we identify the additional roots α_C (see Definition 1.3) with certain collections C of vertices and edges of G . We use this notation for the other graphs below as well.

FIGURE 4. Additional roots for $(15, 7, 1)$

For $G = K_5$ these collections C of vertices and edges are pictured in Fig. 4:

- (1) 10 (-4) -roots with C an edge, e.g. $C = \{12\}$.
- (2) 15 (-2) -roots with C a vertex and two edges, all disjoint from each other, e.g. $C = \{1, 23, 45\}$.
- (3) 20 (-2) -roots with $C = \{1, 12, 34, 35, 45\}$ etc, with C consisting of three edges in a triangle, an edge disjoint from it, plus a vertex on the latter edge.

The edges between the main and additional roots are specified in Definition 1.3. We now list the typical edges between the additional roots $\alpha_C, \alpha_{C'}$. The others follow by S_5 -symmetry.

- (1) α_{12} is connected by a single line to α_{34} ; by a double line to $\alpha_{3,14,25}$; and by a broken line to $\alpha_{3,13,24,25,45}$.
- (2) $\alpha_{1,23,45}$ is connected by a double line to α_{24} ; a bold line to $\alpha_{1,24,35}, \alpha_{2,13,45}, \alpha_{1,12,34,35,45}$ and $\alpha_{2,14,15,23,45}$; and a broken line to $\alpha_{2,14,35}, \alpha_{2,12,34,35,45}$ and $\alpha_{2,13,14,25,34}$.
- (3) $\alpha_{1,12,34,35,45}$ a bold line to $\alpha_{1,23,45}$ and $\alpha_{3,12,45}$; and a broken line to $\alpha_{23}, \alpha_{2,13,45}, \alpha_{3,14,25}, \alpha_{1,13,24,25,45}, \alpha_{2,12,34,35,45}, \alpha_{3,12,15,25,34}, \alpha_{3,14,15,23,45}, \alpha_{2,14,15,23,45}$, and $\alpha_{3,13,24,25,45}$.

The entire intersection matrix can be easily described as follows. The main roots $\alpha_1^m, \alpha_{12}^m$ etc. form a basis of the lattice S . Let ω_1 and ω_{12} etc. denote the vectors such that $\alpha_I^m \cdot \omega_J = 2\delta_{IJ}$, i.e. forming twice the dual basis. Then $\alpha_C = \sum_{I \in C} \omega_I$, where I is one of the sets $1, \dots, 5, 12, \dots, 45$. Thus, it suffices to specify the typical intersection numbers between ω_I . They are:

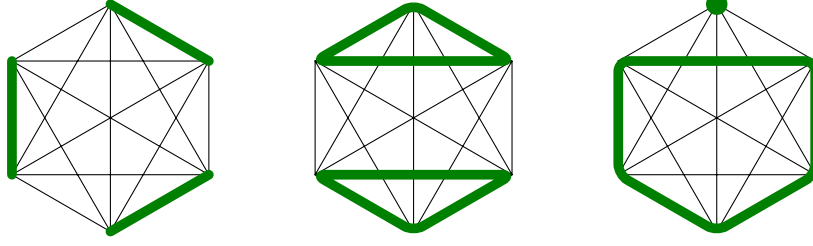
$$\omega_1^2 = -6, \omega_1 \cdot \omega_2 = 2, \omega_1 \cdot \omega_{12} = -2, \omega_1 \cdot \omega_{23} = 2, \omega_{12}^2 = -4, \omega_{12} \cdot \omega_{23} = 0, \omega_{12} \cdot \omega_{34} = 2.$$

The (-4) -vectors of Γ_r form the Petersen graph on 10 vertices, with simple edges.

There are 1027 maximal parabolic subdiagrams, and 20 modulo $\text{Aut } \Gamma_r = S_5$:

- (1) odd: $\tilde{E}_7 \tilde{C}_6(2), \tilde{B}_6 \tilde{F}_4 \tilde{C}_3(2), \tilde{B}_6 \tilde{C}_6(2) \tilde{A}_1, \tilde{D}_6 \tilde{C}_5(2) \tilde{C}_2(2), \tilde{B}_8 \tilde{C}_5(2), \tilde{A}_5 \tilde{A}_5(2) \tilde{B}_3, \tilde{F}_4^3 \tilde{A}_1, \tilde{C}_4(2) \tilde{B}_4^2 \tilde{A}_1, \tilde{E}_6 \tilde{E}_6(2) \tilde{A}_1, \tilde{A}_7 \tilde{D}_5(2) \tilde{A}_1, \tilde{D}_4 \tilde{C}_3^3(2).$
- (2) even ordinary: $\tilde{E}_7 \tilde{B}_5(2) \tilde{A}_1, \tilde{D}_8 \tilde{B}_4(2) \tilde{A}_1, \tilde{E}_8 \tilde{B}_5(2), \tilde{C}_8 \tilde{F}_4(2) \tilde{A}_1, \tilde{E}_7 \tilde{F}_4(2) \tilde{C}_2, \tilde{D}_6 \tilde{C}_4 \tilde{B}_3(2), \tilde{A}_9 \tilde{A}_4(2), \tilde{C}_6^2 \tilde{A}_1, \tilde{C}_{10} \tilde{B}_3(2).$

(16, 6, 1). Γ_r contains 118 roots. The starting graph G is K_6 , a complete graph on 6 vertices. As in Definition 1.3, the subdiagram of the main roots is $K_6^{(2)}$. It has 6 (-2) -roots corresponding to vertices of K_6 —call them 1, 2, 3, 4, 5, 6—and 15 (-2) -roots corresponding to the edges of K_6 —call them 12, 13 etc, for a total of 21 main roots. Let us denote the main roots $\alpha_1^m, \alpha_{12}^m$ etc.

FIGURE 5. Additional roots for $(16, 6, 1)$

The additional roots α_C correspond to the following collections of vertices and edges of the starting graph G , pictured in Fig. 5, modulo S_6 :

- (1) 15 (-4) -roots $\alpha_{12,34,56}$ for C equal to a triple of disjoint edges.
- (2) 10 (-4) -roots $\alpha_{12,23,31,45,56,64}$ for C equal to the 6 edges in two disjoint triangles.
- (3) 72 (-2) -roots $\alpha_{12,23,34,45,51,6}$ for a cycle of 5 edges and a vertex.

The 15 main roots α_{12} for the edges, together with $\alpha^m = \alpha_1^m + \alpha_2^m + \dots + \alpha_6^m$ span the lattice over \mathbb{Q} . Let $\omega_{12}, \dots, \omega_{56}, \omega$ be twice the dual basis. Then the additional roots are $\alpha_C = \sum_{I \in C} \omega_I$, where we formally set $\omega_1 = \omega$ etc for the vertices. The multiplication table for this dual basis is very easy: $\omega_{12}^2 = -\frac{16}{9}$ for the edges, and all the other products and squares are $\frac{2}{9}$. Thus,

$$\omega_C \cdot \omega_{C'} = \frac{2}{9} |C| \cdot |C'| - 2 |C \cap C' \cap \text{Edges}(G)|.$$

Explicitly, the edges between the additional roots are:

- (1) Two roots of type (1) are joined by a bold line if they don't share an edge.
- (2) Two roots of type (2) are joined by a bold line.
- (3) Two roots of type (3) are joined by a bold line if they share 3 edges, and by a broken line otherwise.
- (4) Roots of types (1) and (2) are joined by a bold line if they don't share an edge, by a single line if they share one edge.
- (5) Roots of types (1) and (3) are joined by a broken line if they don't share edges, and by a double line if they share one edge.
- (6) Roots of types (2) and (3) are joined by a double line if they share three edges, and by a broken line if they share fewer edges.

The 15 additional roots α_{12} etc. for the edges are mutually orthogonal (-2) -roots. Denote by $v = \alpha_1^m + \dots + \alpha_6^m$ the sum of the main roots for the vertices of K_6 and by $e = \alpha_{12}^m + \dots + \alpha_{56}^m$ the sum of the main roots for the edges of K_6 . Then $h = \frac{1}{3}(v + e)$ is a vector in H satisfying $h^2 = 2$ and orthogonal to the above 15 roots. Then $h, \alpha_{12}, \dots, \alpha_{56}$ form a sublattice of H isomorphic to $I_{1,15}(2)$. Thus, H can be identified with an S_6 -symmetric lattice lying between it and its dual $I_{1,15}(\frac{1}{2})$.

With the control vector $v_0 = h$, Vinberg's algorithm terminates in four steps.

There are 8917 maximal parabolic subdiagrams, 28 modulo $\text{Aut } \Gamma_r = S_6$:

- (1) odd: $\tilde{B}_6 \tilde{C}_4(2) \tilde{B}_4, \tilde{B}_{10} \tilde{C}_4(2), \tilde{B}_6^2 \tilde{C}_2(2), \tilde{E}_8 \tilde{C}_6(2), \tilde{D}_6 \tilde{B}_4 \tilde{C}_3(2) \tilde{A}_1, \tilde{D}_8 \tilde{C}_4(2) \tilde{C}_2(2), \tilde{E}_6 \tilde{A}_5(2) \tilde{B}_3, \tilde{B}_8 \tilde{F}_4 \tilde{C}_2(2), \tilde{B}_8 \tilde{C}_6(2), \tilde{B}_6 \tilde{F}_4^2, \tilde{E}_7 \tilde{F}_4 \tilde{C}_3(2), \tilde{E}_7 \tilde{C}_5(2) \tilde{C}_2(2), \tilde{D}_6 \tilde{C}_3^2(2) \tilde{C}_2(2), \tilde{D}_4 \tilde{C}_2^3(2), \tilde{A}_5^2 \tilde{A}_2^2(2), \tilde{A}_7 \tilde{A}_3(2) \tilde{B}_3 \tilde{A}_1(2), \tilde{B}_4^3 \tilde{C}_2(2), \tilde{A}_9 \tilde{A}_4(2) \tilde{A}_1.$

- (2) even ordinary: $\tilde{E}_8\tilde{F}_4(2)\tilde{C}_2$, $\tilde{D}_{10}\tilde{B}_3(2)\tilde{A}_1$, $\tilde{C}_{10}\tilde{F}_4(2)$, $\tilde{E}_7\tilde{C}_4\tilde{B}_3(2)$, $\tilde{C}_{12}\tilde{C}_2$, $\tilde{D}_8\tilde{C}_4\tilde{C}_2$, $\tilde{A}_{11}\tilde{A}_2(2)\tilde{A}_1(2)$, $\tilde{E}_7\tilde{C}_6\tilde{A}_1$, $\tilde{C}_8\tilde{C}_6$, $\tilde{D}_6^2\tilde{C}_2$.

Prof. Shigeru Mukai has informed me that this Coxeter diagram can also be obtained as a face of the fundamental polyhedron for the lattice $(A_3 \oplus A_1^6)^\perp$ in $II_{1,25}$ which was computed by Kondō [Kon98] using the Borcherds method [Bor87].

(18, 4, 0). The diagram Γ_r was described by Keum and Kondō [KK01] using the method of [Bor87] and the Leech lattice. Our description is quite different. The Borcherds method does not always produce the Coxeter diagram of a reflexive lattice (e.g. it does not in the (16, 6, 1) case). So the equivalence between our diagram and Keum-Kondō's is not immediate. But it can be checked directly.

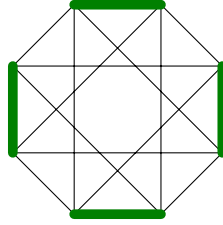


FIGURE 6. Additional roots for (18, 4, 0)

The Coxeter diagram Γ_r contains 48 roots. The starting graph is $G = K_{4,4}$, the complete bipartite graph on 8 vertices, shown in Figure 6. As in Definition 1.3, the subdiagram of the main roots is $K_{4,4}^{(2)}$. It has 8 (-2) -roots corresponding to the vertices of $K_{4,4}$ and 16 (-2) -roots corresponding to the edges of $K_{4,4}$, for a total of 24 main roots.

The additional 24 (-4) -roots α_C are in bijection with the sets of four disjoint edges in G , i.e. with the perfect matchings on the set of vertices of G . The intersection numbers are $\alpha_C \cdot \alpha_{C'} = 4 - 2|C \cap C'|$. Thus, α_C and $\alpha_{C'}$ are connected by a bold line if they don't share any edges, and by a single line if they share exactly one edge. Via a natural bijection between the perfect matchings in $K_{4,4}$ and elements of the group S_4 , $C \cap C'$ is the set of fixed points of $C^{-1} \circ C' \in S_4$.

The graph $K_{4,4}$ is bipartite, its vertices are split into two groups of four. Denote by $v^{(1)}$, resp. $v^{(2)}$, the sum of the main roots in the first, resp. the second group. Denote by e the sum of the main roots for the 16 edges. Then $a = \frac{1}{4}(2v^{(1)} + e)$ and $b = \frac{1}{4}(2v^{(2)} + e)$ are two vectors in H satisfying $a^2 = b^2 = 0$, $a \cdot b = 4$. They are also orthogonal to the 16 main (-2) -roots α_{ij}^m for the edges, which are mutually orthogonal as well. Together they form a standard basis of the sublattice $(I_{0,16} \oplus U)(2)$ in H . Thus, H can be identified with an $(\text{Aut } K_{4,4})$ -invariant lattice lying between it and its dual $(I_{0,16} \oplus U)(\frac{1}{2})$.

With the control vector $v_0 = a + b$, Vinberg's algorithm terminates in two steps.

The automorphism group of the diagram is $\text{Aut } \Gamma_r = \text{Aut } K_{4,4} = S_2 \ltimes (S_4 \times S_4)$. There are 5244 maximal parabolic subgraphs, 17 modulo $\text{Aut } \Gamma_r$:

- (1) odd: $\tilde{D}_8\tilde{B}_4^2$, $\tilde{E}_8\tilde{F}_4^2$, $\tilde{E}_7\tilde{B}_6\tilde{C}_3(2)$, $\tilde{A}_{11}\tilde{B}_3\tilde{A}_2(2)$, $\tilde{E}_6^2\tilde{A}_2^2(2)$, $\tilde{B}_{12}\tilde{F}_4$, $\tilde{D}_6^2\tilde{C}_2^2(2)$, $\tilde{D}_{10}\tilde{C}_3^2(2)$, \tilde{B}_8^2 , $\tilde{A}_7^2\tilde{A}_1^2(2)$, \tilde{D}_4^4 .
(2) even ordinary: $\tilde{A}_{15}\tilde{A}_1(2)$, $\tilde{E}_7^2\tilde{C}_2$, $\tilde{D}_{12}\tilde{C}_4$, $\tilde{C}_8\tilde{E}_8$, \tilde{C}_{16} , \tilde{D}_8^2 .

(20, 2, 1). The Coxeter diagram was computed by Vinberg and Kaplinskaja in [VK78], see also [Vin83]. For easier comparison with the above diagrams we list the roots in Figure 7. There are 25 main roots for the vertices and edges of the Petersen's graph and 25 additional roots: 20 (-2) -roots of the first kind and 5 (-4) -roots of the second kind.

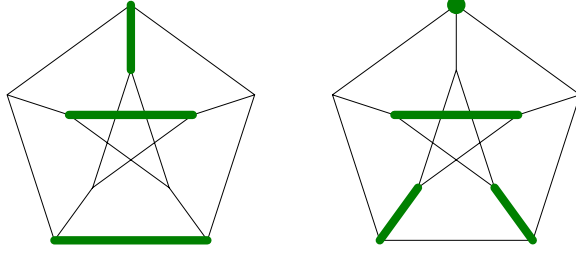


FIGURE 7. Additional roots for $(20, 2, 1)$

There are 581 maximal parabolic subdiagrams, 13 modulo $\text{Aut } \Gamma_r = S_5$, all odd: $\tilde{B}_{18}, \tilde{B}_{10}\tilde{E}_8, \tilde{D}_{16}\tilde{C}_2(2), \tilde{D}_{10}\tilde{E}_7\tilde{A}_1, \tilde{E}_8^2\tilde{C}_2(2), \tilde{E}_7^2\tilde{B}_4, \tilde{D}_{12}\tilde{B}_6, \tilde{D}_8^2\tilde{C}_2(2), \tilde{A}_9^2, \tilde{A}_{15}\tilde{B}_3, \tilde{A}_{11}\tilde{E}_6\tilde{A}_1(2), \tilde{A}_{17}\tilde{A}_1, \tilde{D}_6^3$. On the unique K3 surface with this Picard lattice they define 13 types of elliptic pencils with a section. The rules of Fig. 2 lead to a description of the Kodaira types of the singular fibers in these pencils.

(13, 11, 1). Γ_r has 16 roots. There are 9 maximal parabolic subdiagrams, 5 modulo $\text{Aut } \Gamma_r = S_2$:

- (1) odd: $\tilde{C}_{11}(2), \tilde{E}_8(2)\tilde{C}_3(2),$
- (2) even ord: $\tilde{B}_8(2)\tilde{B}_3(2), \tilde{B}_7(2)\tilde{F}_4(2), \tilde{E}_7(2)\tilde{C}_3\tilde{A}_1.$

(14, 10, 1). Γ_r has 21 roots, There are 69 maximal parabolic subdiagrams, 12 modulo $\text{Aut } \Gamma_r = D_6$:

- (1) odd: $\tilde{C}_8(2)\tilde{F}_4, \tilde{E}_7(2)\tilde{B}_3\tilde{C}_2(2), \tilde{C}_8(2)\tilde{C}_4(2), \tilde{D}_8(2)\tilde{C}_4(2),$
- (2) even ord: $\tilde{B}_4(2)\tilde{B}_4(2)\tilde{B}_4(2), \tilde{C}_6\tilde{B}_6(2), \tilde{B}_6(2)\tilde{C}_4\tilde{C}_2, \tilde{B}_4(2)\tilde{F}_4(2)\tilde{F}_4(2), \tilde{D}_6(2)\tilde{C}_3\tilde{C}_3, \tilde{E}_6(2)\tilde{A}_5\tilde{A}_1,$
- (3) even char: $\tilde{E}_7(2)\tilde{C}_5, \tilde{B}_8(2)\tilde{F}_4(2).$

(15, 9, 1). Γ_r has 98 roots which modulo $\text{Aut } \Gamma_r = \text{PGL}(2, 7)$ of order 336 split into four orbits of sizes 14, 14, 14, 56. The first group of 14 forms the subdiagram G of the main roots. Here, G is a 4-regular bipartite graph on 14 vertices. It has a natural embedding into the complete bipartite graph $K_{7,7}$. G is the co-Heawood graph; its edges in $K_{7,7}$ are complementary to the edges of the well known Heawood graph, a 3-regular graph on 14 vertices. One way to describe G is to say that its vertices correspond to the points and lines in the Fano plane \mathbb{P}^2 over \mathbb{F}_2 , and that a line and a point are joined by an edge iff they are *not* incident.

The remaining roots are additional. They are connected to the main roots by 1, 4 and 6 edges. The first of these groups is formed by the (-4) -roots. This subdiagram is isomorphic to the Heawood graph. Each of these roots is connected to exactly one main root and $\alpha_i^m \alpha_i = 4$. The remaining two orbits are formed by the (-2) -roots of divisibility 2. By [AE22, Lem. 4.14] removing one of these roots

and its (-2) -neighbors gives the Coxeter diagrams for the lattices $(14, 8, 0)$ and $(14, 8, 1)$.

There are 2114 maximal parabolic subdiagrams, and 20 modulo $\text{Aut } \Gamma_r = \text{Aut } G$:

- (1) odd: $\tilde{D}_6(2)\tilde{B}_3^2\tilde{A}_1, \tilde{A}_7(2)\tilde{A}_3\tilde{C}_3(2), \tilde{E}_6(2)\tilde{A}_5\tilde{C}_2(2), \tilde{C}_6(2)\tilde{B}_4\tilde{C}_3(2), \tilde{C}_4^3(2)\tilde{A}_1, \tilde{E}_7(2)\tilde{B}_5\tilde{A}_1, \tilde{C}_8(2)\tilde{F}_4\tilde{A}_1, \tilde{C}_7(2)\tilde{B}_6, \tilde{C}_5(2)\tilde{F}_4^2.$
- (2) even ord: $\tilde{A}_7\tilde{D}_5(2)\tilde{A}_1, \tilde{E}_6\tilde{E}_6(2)\tilde{A}_1, \tilde{C}_4^2\tilde{B}_4(2)\tilde{A}_1, \tilde{D}_4\tilde{B}_3^3(2), \tilde{F}_4^3(2)\tilde{A}_1, \tilde{C}_8\tilde{B}_5(2), \tilde{A}_5\tilde{A}_5(2)\tilde{C}_3, \tilde{E}_7\tilde{B}_6(2), \tilde{C}_6\tilde{F}_4(2)\tilde{B}_3(2), \tilde{D}_6\tilde{B}_5(2)\tilde{C}_2, \tilde{C}_6\tilde{B}_6(2)\tilde{A}_1.$

Note that $(15, 9, 1) \simeq \langle -2 \rangle \oplus (14, 8, 1) \simeq \langle -2 \rangle \oplus (14, 8, 0)$. Among these two, $(14, 8, 1) = S_X$ for some K3 surface with a nonsymplectic involution, and $(15, 9, 1)$ is the Picard lattice of the hyperkahler manifold $\text{Hilb}^2(X)$. The symmetry group of the Coxeter diagram $\Gamma_r(14, 8, 1)$ is only S_4 , so in this case $\text{Hilb}^2(X)$ is much more symmetric than the K3 surface X .

(18, 6, 0). The Coxeter diagram Γ_r was described by Borchers [Bor00] and it consists of 64 + 896 roots. I computed the maximal parabolic subdiagrams of Γ_r . There are 90897634 of them, 28 modulo the group $\text{Aut } \Gamma_r$ of order $2^{16} \cdot 3^2 \cdot 5 \cdot 7$:

- (1) odd: $\tilde{B}_8\tilde{F}_4^2, \tilde{E}_7\tilde{C}_5(2)\tilde{F}_4, \tilde{C}_8(2)\tilde{E}_8, \tilde{D}_8\tilde{C}_4(2)^2, \tilde{B}_6^2\tilde{C}_4(2), \tilde{E}_6\tilde{A}_5(2)\tilde{B}_5, \tilde{B}_4^4, \tilde{B}_{10}\tilde{C}_6(2), \tilde{D}_6\tilde{B}_4\tilde{C}_3(2)^2, \tilde{D}_9\tilde{A}_7(2), \tilde{A}_9\tilde{A}_4(2)\tilde{C}_3(2), \tilde{A}_5^2\tilde{C}_2(2)\tilde{A}_2(2)^2, \tilde{D}_5^2\tilde{A}_3(2)^2, \tilde{A}_7\tilde{A}_3(2)\tilde{B}_3^2, \tilde{D}_4^2\tilde{C}_2(2)^4, \tilde{A}_3^4\tilde{A}_1(2)^4, \tilde{A}_1^{16}.$
- (2) even ord: $\tilde{E}_7\tilde{C}_6\tilde{B}_3(2), \tilde{D}_{10}\tilde{B}_3(2)^2, \tilde{C}_{12}\tilde{F}_4(2), \tilde{E}_8\tilde{F}_4(2)^2, \tilde{D}_8\tilde{C}_4^2, \tilde{D}_6^2\tilde{C}_2^2, \tilde{C}_8^2, \tilde{A}_{11}\tilde{C}_3\tilde{A}_2(2), \tilde{E}_6^2\tilde{A}_2(2)^2, \tilde{A}_7^2\tilde{A}_1(2)^2, \tilde{D}_4^4.$

(22, 2, 0). The Coxeter diagram Γ_r was described by Borchers [Bor87] and by Dolgachev-Kondō [DK03]. It consists of 42 main (-2) -roots corresponding to the 21 points and 21 lines of $\mathbb{P}^2(\mathbb{F}_4)$, and 168 additional (-4) -roots. $\text{Aut } \Gamma_r = \text{PSL}(3, \mathbb{F}_4).D_6$ has order 241920. By Esselmann [Ess96] this lattice has the maximal possible rank for a reflective hyperbolic lattice.

I computed the maximal parabolic subdiagrams of Γ_r . There are 1095990 of them, 18 modulo $\text{Aut } \Gamma_r$, all odd: $\tilde{E}_7^2\tilde{B}_6, \tilde{E}_8^2\tilde{F}_4, \tilde{A}_7^2\tilde{D}_5\tilde{A}_1(2), \tilde{D}_{12}\tilde{B}_8, \tilde{B}_{20}, \tilde{B}_{12}\tilde{E}_8, \tilde{D}_6^3\tilde{C}_2(2), \tilde{D}_{16}\tilde{F}_4, \tilde{D}_{10}\tilde{E}_7\tilde{C}_3(2), \tilde{D}_8^2\tilde{B}_4, \tilde{A}_{15}\tilde{B}_5, \tilde{A}_9^2\tilde{C}_2(2), \tilde{A}_{11}\tilde{E}_6\tilde{B}_3, \tilde{A}_{11}\tilde{D}_7\tilde{A}_2(2), \tilde{A}_{17}\tilde{C}_3(2), \tilde{E}_6^3\tilde{A}_2(2), \tilde{A}_5^4, \tilde{D}_4^5.$

(14, 12, 1). Γ_r has 17 roots. There are 16 maximal parabolic subdiagrams, 9 modulo $\text{Aut } \Gamma_r = S_2$:

- (1) odd: $\tilde{E}_8(2)\tilde{C}_4(2), \tilde{C}_{12}(2), \tilde{D}_{12}(2),$
- (2) even ord: $\tilde{D}_8(2)\tilde{B}_4(2), \tilde{B}_8(2)\tilde{B}_4(2), \tilde{B}_8(2)\tilde{F}_4(2), \tilde{E}_7(2)\tilde{C}_3\tilde{C}_2,$
- (3) even char: $\tilde{E}_8(2)\tilde{F}_4(2), \tilde{B}_{12}(2).$

(15, 11, 1). There are 66 roots which modulo $\text{Aut } \Gamma_r = S_2 \times (S_3 \times S_3)$ split into five orbits. The subdiagram of the main roots is the graph $L(K_{3,3})$, the line graph of $K_{3,3}$, a 4-regular on 9 vertices. The other roots are additional.

The (-4) -roots are split into two groups of sizes 6, and 9, connected to the main roots by 0, resp. 2 edges. Together, they form the graph $K_{3,3}^{(2)}$. There are also two orbits of sizes 6 and 36 connected to the main roots by 3, resp. 5 edges, latter with multiplicities 2, 2, 2, 4, 4. These are (-2) -roots of divisibility 2. By [AE22, Lem. 4.14] removing one of these roots and its (-2) -neighbors gives the Coxeter diagrams for the lattices $(14, 10, 0)$ and $(14, 10, 1)$.

There are 522 maximal parabolic subdiagrams, 16 modulo $\text{Aut } \Gamma_r = \text{Aut } G$:

- (1) odd: $\tilde{A}_{11}(2)\tilde{A}_2, \tilde{E}_7(2)\tilde{C}_3(2)\tilde{B}_3, \tilde{C}_{12}(2)\tilde{A}_1, \tilde{E}_8(2)\tilde{F}_4\tilde{A}_1, \tilde{C}_8(2)\tilde{C}_5(2), \tilde{C}_9(2)\tilde{F}_4, \tilde{D}_8(2)\tilde{C}_4(2)\tilde{A}_1.$
- (2) even ord: $\tilde{E}_6(2)\tilde{A}_5\tilde{C}_2, \tilde{B}_6(2)\tilde{C}_4\tilde{B}_3(2), \tilde{A}_7(2)\tilde{B}_3(2)\tilde{A}_3, \tilde{B}_7(2)\tilde{C}_6, \tilde{B}_4^3(2)\tilde{A}_1, \tilde{D}_6(2)\tilde{C}_3^2\tilde{A}_1, \tilde{B}_8(2)\tilde{F}_4(2)\tilde{A}_1, \tilde{E}_7(2)\tilde{C}_5\tilde{A}_1, \tilde{B}_5(2)\tilde{F}_4^2(2).$

(15, 13, 1). Γ_r has 27 roots. There are 46 maximal parabolic subdiagrams, 10 modulo $\text{Aut } \Gamma_r = S_3$:

- (1) odd: $\tilde{E}_8(2)\tilde{C}_5(2), \tilde{D}_{12}(2)\tilde{A}_1, \tilde{C}_{13}(2),$
- (2) even ord: $\tilde{E}_7(2)\tilde{C}_3\tilde{B}_3(2), \tilde{B}_8(2)\tilde{B}_5(2), \tilde{A}_{11}(2)\tilde{A}_2, \tilde{B}_{12}(2)\tilde{A}_1, \tilde{B}_9(2)\tilde{F}_4(2), \tilde{D}_8(2)\tilde{B}_4(2)\tilde{A}_1, \tilde{E}_8(2)\tilde{F}_4(2)\tilde{A}_1.$

(16, 12, 1). There are 118 roots which modulo $\text{Aut } \Gamma_r = S_6$ split into five orbits of sizes 15, 15, 6, 10, 72 of vectors with square $-2, -4, -4, -2, -4$. There are 15 main roots forming $L(K_6)$, the line graph of the complete graph K_6 . If $L = (16, 6, 1)$ then $(16, 12, 1)$ is the even sublattice of $L^*(2)$. This implies that the maximal parabolic diagrams of the $(16, 12, 1)$ lattice are in a bijection with those of the $(16, 6, 1)$ lattice, with the (-2) and (-4) -roots interchanged, and odd and even ordinary diagrams interchanged.

(16, 14, 1). There are 29 roots. This diagram is dual to that of $(16, 4, 1)$, with the (-2) and (-4) roots switched. There are 115 maximal parabolic subdiagrams, 14 modulo $\text{Aut } \Gamma_r = D_6$:

- (1) odd: $\tilde{E}_8(2)\tilde{C}_6(2), \tilde{C}_{14}(2), \tilde{D}_{12}(2)\tilde{C}_2(2), \tilde{E}_7(2)\tilde{E}_7(2),$
- (2) even ord: $\tilde{E}_8(2)\tilde{F}_4(2)\tilde{C}_2, \tilde{D}_8(2)\tilde{B}_4(2)\tilde{C}_2, \tilde{B}_{12}(2)\tilde{C}_2, \tilde{D}_{10}(2)\tilde{C}_3\tilde{A}_1(2), \tilde{E}_7(2)\tilde{B}_4(2)\tilde{C}_3, \tilde{E}_7(2)\tilde{B}_6(2)\tilde{A}_1(2), \tilde{B}_8(2)\tilde{B}_6(2), \tilde{B}_{10}(2)\tilde{F}_4(2), \tilde{A}_{11}(2)\tilde{A}_2\tilde{A}_1, \tilde{D}_6(2)\tilde{D}_6(2)\tilde{C}_2.$

Other coeven lattices. If $S = (r, a, 0)$ is an even coeven lattice then so is $S^\dagger = S^*(2) = (r, r - a, 0)$. Their Coxeter diagrams are dual, with (-2) and (-4) -roots interchanged, and there is a bijection between the maximal parabolic subdiagrams. The remaining lattices in Fig. 1 are obtained from the ones already listed here or in [AE22]. This applies to the following lattices:

$$(14, 10, 0), (14, 12, 0), (18, 12, 0), (18, 14, 0), (18, 16, 0), (22, 20, 0).$$

4. APPLICATIONS TO INFINITE AUTOMORPHISM GROUPS OF K3 SURFACES

The main application of the Coxeter diagrams in [Vin83] was the description, for the very first time, of two infinite automorphism groups of K3 surfaces. In the same way our computations imply such a description in several more cases.

A K3 surface X whose Picard lattice S_X is 2-elementary comes with a canonical nonsymplectic involution ι on X , acting as $+1$ on S and as -1 on the lattice of transcendental cycles $T = S^\perp$ in L_{K3} . Any automorphism of X commutes with ι . Let $Y = X/\iota$ be the quotient surface. It is a rational surface unless $S = (10, 0, 0)$ in which case Y is an Enriques surface. Let B be the branch divisor of $\pi: X \rightarrow Y$ and denote by $\text{Aut}'(Y, B)$ the subgroup of $\text{Aut}(Y, B)$ acting trivially on $\text{Pic } Y$.

Lemma 4.1. *Let S be a 2-elementary K3 lattice $S \neq (10, 10, 0)$, Γ_r the Coxeter diagram of S , and let X be a K3 surface with Picard lattice $S_X = S$. Then there exists an exact sequence*

$$0 \rightarrow \langle \iota \rangle \times \text{Aut}'(Y, B) \rightarrow \text{Aut } X \rightarrow \text{Sym } \Gamma_r \ltimes W(\Gamma_4) \rightarrow 0,$$

Lattice	$\text{Aut } \Gamma_r$	Γ_4
(11, 11, 1)	1	$T_{2,3,7}$
(12, 10, 1)	1	$T_{2,4,6} \sqcup A_1$
(13, 9, 1)	S_3	$T_{4,4,4}$
(14, 8, 1)	S_4	a 10-vertex trivalent tree with 6 ends
(15, 7, 1)	S_5	the Petersen graph
(16, 6, 1)	S_6	a diagram with 10 + 15 vertices
(18, 4, 0)	$S_2 \ltimes (S_4 \times S_4)$	a diagram with 24 vertices
(20, 2, 1)	S_5	K_5 with bold edges

TABLE 1. Coxeter diagrams Γ_4 defining $\text{Aut } X$

where $\Gamma_4 \subset \Gamma_r$ is the subdiagram formed by the (-4) -roots, and $W(\Gamma_4)$ is the corresponding Coxeter group.

Proof. A well-known application of Torelli theorem [PSS71] says that for a projective K3 surface with an ample cone $A(X)$ the natural homomorphism

$$\rho: \text{Aut } X \rightarrow \text{Aut } A(X) = O^+(S)/W_2(S) = O(S)/\pm W_2(S),$$

has finite kernel and cokernel. The kernel of ρ consists of automorphisms that act trivially on S_X . They descend to automorphisms of the pair (Y, B) , and ι is the only one descending to the identity. Vice versa, an automorphism of (Y, B) lifts to an automorphism of X since $X = \text{Spec } \mathcal{O} \oplus L^{-1}$ with $L^2 \simeq \mathcal{O}(B)$ and $\text{Pic } Y$ has no 2-torsion. $(\text{Pic } Y) \otimes \mathbb{Q}$ is identified with $(\text{Pic } X)^\iota \otimes \mathbb{Q} = S \otimes \mathbb{Q}$. So, the automorphisms of X acting trivially on S descend to $\text{Aut}'(Y, D)$. Thus, $\ker \rho = \mathbb{Z}_2 \times \text{Aut}(Y, B)$.

The homomorphism ρ is surjective. Indeed, an isometry of L_{K3} is equivalent to a pair of isometries of S and T which have the same image in the finite isometry group of the discriminant group under $O(S) \rightarrow O(A_S, q_S) = O(A_T, q_T) \leftarrow O(T)$. By [Nik79] for an indefinite 2-elementary lattice H , such as S and T , the homomorphism $O(H) \rightarrow O(A_H, q_H)$ is surjective. So any element of $O(S)$ can be lifted to $a \in O(L_{K3})$. Then a composition $w \circ a$ with some $w \in W_2(S)$ sends the fundamental domain $A(X)$ to itself and therefore is induced by some $g \in \text{Aut } X$.

By [Vin83, Prop., p.2] or [AN06, Prop. 2.4] the quotient group $W(\Gamma_r)/W_2(S)$ is isomorphic to $W(\Gamma_4)$. Together with the equality $O^+(S) = \text{Sym } \Gamma_r \ltimes W(\Gamma_r)$ this gives $O^+(S)/W_2(S) = \text{Sym } \Gamma_r \ltimes W(\Gamma_4)$. \square

By [AE22, Sec. 3], for the 2-elementary K3 lattices on the $r + a = 20$ line the groups $\text{Sym } \Gamma_r \ltimes W(\Gamma_4)$ are extensions of affine groups $W(\tilde{E}_n)$ by dihedral groups. The diagrams of this paper provide even more interesting examples. The (-4) -subdiagrams for the K3 lattices with $r + a = 22$ were given in the previous section. We list them in Table 1. $T_{p,q,r}$ denotes a tree with legs of lengths p, q, r .

The diagrams Γ_4 for $(16, 6, 1)$ and $(18, 4, 0)$ are quite complicated, and have both simple and bold edges. It is a little easier to describe the subdiagram Γ'_4 of Γ_4 with the bold edges removed. The Coxeter group $W(\Gamma'_4)$ is the quotient of $W(\Gamma_4)$ by the additional commuting relations for the bold edges.

For $(16, 6, 1)$ the graph Γ'_4 is a union of 10 disjoint vertices and $L(K_6)$.

For $(18, 4, 0)$ the graph Γ'_4 is a union of two disjoint subgraphs $G_1 \sqcup G_2$, and each G_i can be defined as the complement of $K_4 \sqcup K_4 \sqcup K_4$ in the complete graph K_{12} : an edge of K_{12} is in G_i iff it is not in $K_4 \sqcup K_4 \sqcup K_4$. The two 12-element sets

can be identified with the cosets of A_4 in S_4 and the three 4-element sets with the cosets of the Klein four-group V_4 in A_4 .

REFERENCES

- [AE22] Valery Alexeev and Philip Engel, *Mirror symmetric compactifications of moduli spaces of K3 surfaces with a nonsymplectic involution*, [arXiv:2208.10383](#) (2022).
- [AN06] Valery Alexeev and Viacheslav V. Nikulin, *Del Pezzo and K3 surfaces*, MSJ Memoirs, vol. 15, Mathematical Society of Japan, Tokyo, 2006, [arXiv:math/0406536](#).
- [Bor87] Richard Borcherds, *Automorphism groups of Lorentzian lattices*, J. Algebra **111** (1987), no. 1, 133–153.
- [Bor00] Richard E. Borcherds, *Reflection groups of Lorentzian lattices*, Duke Math. J. **104** (2000), no. 2, 319–366.
- [DK03] I. Dolgachev and S. Kondō, *A supersingular K3 surface in characteristic 2 and the Leech lattice*, Int. Math. Res. Not. (2003), no. 1, 1–23.
- [Ess96] Frank Esselmann, *Über die maximale Dimension von Lorentz-Gittern mit coendlicher Spiegelungsgruppe*, J. Number Theory **61** (1996), no. 1, 103–144.
- [KK01] Jonghae Keum and Shigeyuki Kondō, *The automorphism groups of Kummer surfaces associated with the product of two elliptic curves*, Trans. Amer. Math. Soc. **353** (2001), no. 4, 1469–1487.
- [Kon98] Shigeyuki Kondō, *The automorphism group of a generic Jacobian Kummer surface*, J. Algebraic Geom. **7** (1998), no. 3, 589–609.
- [Nik79] V. V. Nikulin, *Integer symmetric bilinear forms and some of their geometric applications*, Izv. Akad. Nauk SSSR Ser. Mat. **43** (1979), no. 1, 111–177, 238.
- [PSS71] I. I. Pjateckiĭ-Shapiro and I. R. Shafarevič, *Torelli’s theorem for algebraic surfaces of type K3*, Izv. Akad. Nauk SSSR Ser. Mat. **35** (1971), 530–572.
- [Sag22] Sage Developers, *Sagemath, the Sage Mathematics Software System (Version 9.5)*, 2022, <https://www.sagemath.org>.
- [Vin72] È. B. Vinberg, *The groups of units of certain quadratic forms*, Mat. Sb. (N.S.) **87(129)** (1972), 18–36.
- [Vin75] È. B. Vinberg, *Some arithmetical discrete groups in Lobačevskii spaces*, Discrete subgroups of Lie groups and applications to moduli (Internat. Colloq., Bombay, 1973), Oxford Univ. Press, Bombay, 1975, pp. 323–348.
- [Vin83] È. B. Vinberg, *The two most algebraic K3 surfaces*, Math. Ann. **265** (1983), no. 1, 1–21.
- [VK78] È. B. Vinberg and I. M. Kaplinskaja, *The groups $O_{18,1}(Z)$ and $O_{19,1}(Z)$* , Dokl. Akad. Nauk SSSR **238** (1978), no. 6, 1273–1275.

Email address: valery@uga.edu

DEPARTMENT OF MATHEMATICS, UNIVERSITY OF GEORGIA, ATHENS GA 30602, USA